Hindawi
Journal of Analytical Methods in Chemistry
Volume 2022, Article ID 9425334, 11 pages
https://doi.org/10.1155/2022/9425334

Research Article

Adsorptive Removal of Azo Dye New Coccine Using High-Performance Adsorbent-Based Polycation-Modified Nano-Alpha Alumina Particles

Thi Hai Yen Doan,[1] **Hong Anh Pham**,[2] **Ngoc Huyen Nguyen**,[2] **Thi Dung Le**,[1] **Thanh Binh Nguyen**,[1] **and Thanh Son Le**[1]

[1]*Faculty of Chemistry, University of Science, Vietnam National University, Hanoi-19 Le Thanh Tong, Hoan Kiem, Hanoi, Vietnam*
[2]*Nguyen Sieu High School, Yen Hoa, Cau Giay, Hanoi, Vietnam*

Correspondence should be addressed to Thi Hai Yen Doan; doanthihaiyen110590@gmail.com

Received 13 December 2021; Revised 6 January 2022; Accepted 15 January 2022; Published 7 February 2022

Academic Editor: Arun Srivastav

The azo dyes new coccine (NCC) were successfully removed through the adsorption onto PVBTAC-modified α-Al_2O_3 particles. The optimal conditions of both the surface modification by PVBTAC adsorption and the NCC adsorption were thoroughly investigated. Formerly, polycations PVBTAC were adsorbed onto the nanosized α-Al_2O_3 particles at *pH* 8, NaCl 100 mM, with a contact time of 2 h, and initial concentration of 1000 ppm to modify the α-Al_2O_3 surface. Latterly, the NCC adsorptive removal was conducted at *pH* 8, NaCl 10 mM, α-Al_2O_3 adsorbent dosage of 3 mg mL^{-1}, and a contact time of 45 min. Interestingly, the optimal *pH* of 8 potentially applies to treat real wastewater as the environmental *pH* range is often about 7–8. High removal efficiency and adsorption capacity of the NCC azo dyes were, respectively, found to be approximately 95% and 3.17 mg g^{-1} with an initial NCC concentration of 10 ppm. The NCC adsorption on the modified α-Al_2O_3 particles was well fitted with a Freundlich model isotherm. A pseudo-second kinetic was more suitable for the NCC adsorption on the PVBTAC-modified α-Al_2O_3 surface than a pseudo-first kinetic. The NCC adsorptive removal kinetic was also affirmed by the FT-IR spectra, based especially on the changes of functional group stretch vibrations of $-SO_3^-$ group in the NCC molecules and $-N^+(CH_3)_3$ group in the PVBTAC molecules. The high reusability of the α-Al_2O_3 particles was proved to be higher than 50% after four generation times.

1. Introduction

Nowadays, the azo dyes have been diversely used in many industrial applications such as textile, clothing, printing, plastic, and paper productions. The azo dyes that contain a specific group $-N=N-$ are the most popular and estimate to be about 50–70% of annual total dye production [1]. The azo dyes durably exist and are non-degraded in the aquatic environment. Moreover, the effluents from these industries often contain a large dye amount of 10–200 mg L^{-1} [2, 3], which is likely dangerous to the ecosystem and human health, causing biohazard risks such as bioaccumulation and mutagenesis inducing genetical diseases, congenital malformations, or cancer [4–6]. For this reason, the dye elimination from the wastewater is necessary.

The most common dye treatment techniques basing on discoloration are physical, chemical, biological methods, and adsorption [7–12]. For decades, a lot of research on the azo dye demand removal from aqueous solution has been conducted [10, 13]. Among them, new coccine (NCC), well known with another name as Acid Red 18, has been recently taken the interest of scientists. NCC is one of the synthetic organic azo dyes widely used in textile industries. NCC degradation by using the TiO_2 photocatalyst in combination with H_2O_2 in a cavitation reactor was intensified up to 88.1% in comparison to 64.8% obtained in an ultrasonic reactor.

NCC degraded up to 99.6% with the employment of the Fenton reagent combining with UV irradiation (UV/FR) at *pH* 3 and under 30 min of reaction time [14]. Among these techniques, adsorption is more effective with high removal efficiency, and simple and low cost. The use of carbon as an adsorbent seems to be popular. NCC was totally removed (higher than 99% in 10 consecutive cycles) from an aqueous solution through adsorbing on carbon nanotubes coated with chitosan at a high temperature of 323.15 K [15]. A maximum NCC removal efficiency reached 90.83% by adsorption onto the almond shell-synthesized activated charcoal at the optimal *pH* 2 [16]. It was found that the use of carbon nanotubes with multiple walls (MWCNTs) could remove 166.67 mg g^{-1} of the NCC from an aqueous solution at *pH* 3 [17]. On the other hand, other materials are also applied as adsorbents. NCC was removed from wastewater by means of adsorbing onto the powder of zero iron at an acidic condition of *pH* 3 [18]. However, strictly controlled conditions, such as high experimental temperature or/and acidic environment, have been requested as the removal efficiency is still low.

Furthermore, alumina has been well known as a potential adsorbent for organic pollutant treatment. Alpha alumina (α-Al_2O_3) was characterized with a high specific surface area and existed as the most stable form at high temperature among various alumina forms such as beta (β)- and gamma (γ)- [19–21]. Recently, the adsorptive removal potential of the organic pollutants was intensified through modifying the α-Al_2O_3 surface by polyelectrolyte adsorption, even at room temperature, which was previously proved [22–24]. It was found that the sodium dodecyl sulfate (SDS) surfactant was strongly attached to the alpha alumina of a small specific surface area [23]. Continuously, oxytetracycline antibiotic was adsorptively removed with a high removal efficiency of higher than 90% by using SDS-modified α-Al_2O_3 [24]. The modification of surface materials has been demonstrated to increase the total net surface charges, enhancing adsorptive removal of wastewater pollutants through electrostatic interactions [25–28]. The adsorption mechanism of the azo dyes were followed Langmuir [15, 29], Freundlich [15, 30], and two-step models [31], while adsorption kinetics were indicated by first-order and second-order models [18, 32, 33].

In this study, attention was focused on removing NCC via adsorption onto polycation-modified α-Al_2O_3 nanosized particles under different conditions at room temperature. The effectiveness parameters including pH, ionic strength, adsorbent dosage, contact time, and the initial concentration on both α-Al_2O_3 modification process and the NCC removal were comprehensively investigated. The adsorption mechanism was discussed based on both the FT-IR spectra and the general adsorption isotherm models such as Langmuir, Freundlich and two-step. Adsorption kinetics were described by the pseudo-first and -second models.

2. Materials and Methods

2.1. Materials. Nanosized alpha alumina (α-Al_2O_3) particles solvothermaly synthesized following the previous method, were used as adsorbents [34]. Accordingly, to precipitate alumina hydroxide, 4 M sodium hydroxide solution was added to 1 M aluminum nitrate solution, respectively prepared from NaOH pellets and $Al(NO_3)_3$ (analytical reagent, Merk, Germany). The precipitates were dried at 80°C for 24 h after centrifugation and rising to neutral *pH* with ultrapure water. Then, the collected precipitates were transformed to α-Al_2O_3 at high temperature of 1200°C for 12 h. Finally, the α-Al_2O_3 were dried and ground after activating by using the solution of 0.05 M NaOH and rising with ultrapure water several times. A high synthesis yield of the α-Al_2O_3 particles was calculated to be approximately $97.23 \pm 1.43\%$. The α-Al_2O_3 particles synthesized were nanosized at about 27 nm determined by transmission electron microscopy (TEM, H7650, Hitachi, Tokyo, Japan). Homopolymer, poly(vinylbenzyl) trimethylammonium chloride) (PVBTAC) with a molecular weight of 343.45 g mol^{-1} (Hyogo, Japan) was applied as a surface modifier.

The stock PVBTAC solution of 10^4 ppm was prepared for adsorption experiments. New coccine with a molecular weight of 604.46 g mol^{-1} (NCC, purity >82% Merck, Germany) was used as azo dye. The polymer working solutions were diluted from the stock solution. The chemical structures of polycation PVBTAC and the NCC dye were described in Figure 1. The NaCl solutions of 0.1 and 1 M (prepared from analytical reagent NaCl, Merk, Germany) were employed to control ionic strength after filtering through cellulose membranes of 0.2 μm pore size. Meanwhile, the solutions of 0.1 M HCl and 0.1 M NaOH (Merk, Germany) were used to adjust the *pH* of the solution under a pH meter (Hanna, USA). All experimental solutions were prepared with ultrapure water (resistance of 18.2 MΩ cm, Labconco, Kansai, MO, USA).

2.2. Modification of Alpha-Alumina Using Highly Positively Charged Polycation

2.2.1. Alpha-alumina Modification by the PVBTAC Adsorption. The nanosized α-Al_2O_3 particles were strongly shaken for 2 h by an orbital shaker before using. To deaggregate particles, the nanosized α-Al_2O_3 particles were sonicated for 30 min before conducting each experimental modification. To modify the particles, suitable PVBTAC stock solution volumes were added to the nanosized α-Al_2O_3 particles. The modification experiments were carried out for about 2 h by vigorously shaking in investigating conditions of pH and ionic strength. Then, the samples were centrifuged to separate the solid-liquid phases. Finally, the solutions were collected to determine PVBTAC-remaining concentration by ultraviolet-visible (UV-Vis) measurement.

2.2.2. NCC Adsorptive Removal Using PVBTAC-Modified Nanosized α-Al2O3 Particles. The nanosized α-Al_2O_3 particles modified by PVBTAC adsorption at optimal conditions were rinsed with ultrapure water to eliminate excess polycation PVBTAC after centrifuging to release remaining water. Then, these modified materials were used to conduct

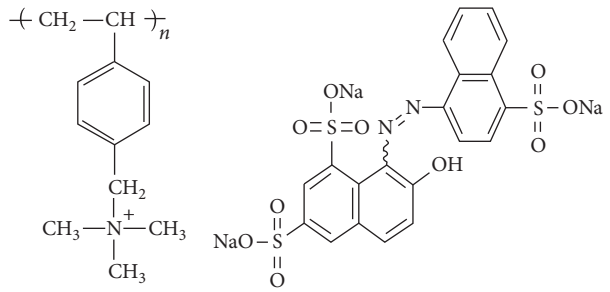

Figure 1: Chemical structures of (a) PVBTAC and (b) NCC.

dye removal experiments at room temperature and different conditional parameters such as *pH*, ionic strength, adsorption time, α-Al_2O_3 adsorbent, and NCC adsorbate dosage. Similarly, the solution was pipetted after centrifugation of the sample. The NCC concentration remaining in the solution was measured by the UV-Vis method. Each experiment was at least triply repeated. Standard deviations were determined by at least triple experiments.

2.3. Methods

2.3.1. Ultraviolet Visible (UV-Vis) Spectroscopy. The PVBTAC and NCC concentrations were determined by an UV-Vis spectroscopy equipped with a spectrophotometer (UV-1650 PC, Shimadzu, Japan) at a wavelength of 224 and 508 nm, respectively.

The PVBTAC adsorption efficiency and the NCC removal efficiency (H, %) were determined

$$H = \frac{C_i - C_e}{C_i} \times 100\%. \tag{1}$$

where C_i and C_e are initial and equilibrium polymer concentrations (ppm), respectively.

The polymer adsorption capacities onto unmodified/modified nanosized α-Al_2O_3 particles were determined by equation (2):

$$\Gamma = \frac{C_i - C_e}{m} \times M \times 1000, \tag{2}$$

where Γ is the polymer adsorption capacity (mg g^{-1}) at contact time t (min), M is polymer molecular weight (g mol^{-1}), and m is the α-Al_2O_3 adsorbent dosage (mg mL^{-1}).

2.3.2. Adsorption Mechanism. The adsorption isotherms of PVBTAC onto the α-Al_2O_3 particles and NCC onto the PVBTAC-modified α-Al_2O_3 particles were considered to be fit with some general adsorption isotherm models such as Langmuir, Freundlich, and two-step [26]. Each adsorption isotherm model was described as below.

First, the Langmuir model described by equation (3) was applicable for absorbate-formed monolayer on the absorbent. The adsorption favorite was evaluated by R_L constant as in equation (4).

$$\frac{C_e}{\Gamma} = \frac{1}{K_L \cdot \Gamma_{\max}} + \frac{C_e}{\Gamma_{\max}}, \tag{3}$$

$$R_L = \frac{1}{1 + K_L \cdot C_i}. \tag{4}$$

where K_L is Langmuir constant.

Second, the concept of the Freundlich model was developed, based on the experimental data, to evaluate that multiple adsorbate layer formed on the inhomogeneous adsorbent surface. It was subjected in

$$\Gamma = K_f \cdot C_e^n, \tag{5}$$

where K_f is Freundlich constant and n is the layer number.

A general equation of the two-step model adsorption isotherm [34] is as follows:

$$\Gamma = \frac{\Gamma_{\max} k_1 C_e \left((1/n) + k_2 C_e^{n-1}\right)}{1 + k_1 C_e \left(1 + k_2 C_e^{n-1}\right)}, \tag{6}$$

where k_1 and k_2 are equilibrium constants for in the first and second adsorption step, respectively.

2.3.3. Adsorption Kinetics. Adsorption kinetics of polymer are often described by the pseudo-first and pseudo-second models proposed by Lagergren as follows [17, 26]:

$$\ln\left(\Gamma_e - \Gamma\right) = \ln\ \Gamma_e - K_1 t,$$
$$\frac{t}{\Gamma} = \frac{1}{K_2 \cdot \Gamma_e^2} + \frac{1}{\Gamma_e} t, \tag{7}$$

where Γ is polymer adsorption capacity at contact time t (mg g^{-1}), Γ_e is the polymer adsorption capacity (mg g^{-1}) at equilibrium state, and K_1 (min^{-1}) and K_2 (g mg^{-1} min^{-1}) are reaction rate constants of the pseudo-first and pseudo-second models, respectively.

2.3.4. Fourier Transform Infrared (FT-IR) Spectroscopy. The mechanisms of adsorption of both PVBTAC onto the α-Al_2O_3 particles and NCC onto the PVBTAC-modified α-Al_2O_3 particles were discussed based on the FT-IR spectra. The PVBTAC adsorption and the NCC adsorption were carried out for 2 h at pH 8 and at ionic strength of NaCl 100 and 10 mM, respectively. Then, the residuals were collected and dried at 80°C after centrifugation and removal of the water excess. Five spectra of the α-Al_2O_3 particles, PVBTAC, NCC, PVBTAC-modified α-Al_2O_3 particles, and NCC-adsorbed-PVBTAC-modified α-Al_2O_3 particles were recorded from 400 to 4000 cm^{-1} by an Affinity-1S spectrophotometer (20 scans averaging, Shimadzu, Japan) at room temperature (293 K).

3. Results and Discussions

3.1. Modification through PVBTAC Adsorption on the Synthesized Nanosized α-Al_2O_3 Particles

3.1.1. pH Effect. The solution *pH* significantly affected the PVBTAC adsorption onto the synthesized nanosized

α-Al_2O_3 particles. To modify the α-Al_2O_3 particles, an initial PVBTAC concentration of 50 ppm was added to the particles of 5 mg mL^{-1} in the *pH* range of 4–12 under different ionic strength conditions of 1, 10, and 100 mM NaCl.

Figure 2 shows that PVBTAC adsorption capacity (Γ_{PVBTAC}) increased with increasing *pH* until *pH* reached 8, then Γ_{PVBTAC} decreased with continuous increment of the *pH*. The α-Al_2O_3 particles were characterized with −O and OH functional groups [19] and an isoelectric point (IEP) of approximately 6.7 [35]. It means that the charging sign of the α-Al_2O_3 particles changed over the IEP point. At the *pH* higher than 6.7, the α-Al_2O_3 particle surface was negatively charged due to the presence of O^- groups while PVBTAC was positively charged, independently from the *pH* level. Therefore, the PVBTAC adsorption onto the α-Al_2O_3 particles was promoted due to electrostatic attractions at the solution *pH* greater than 6.7. Oppositely, at a *pH* lower than 6.7, the α-Al_2O_3 particle surface was positively charged due to appearance of the OH_2^+ groups. These surface groups introduced the strong electrostatic repulsions between PVBTAC molecules and the α-Al_2O_3 surface, resulting in the limitation of the PVBTAC adsorption. At the solution pH of 8, the Γ_{PVBTAC} achieved maximum value at all ionic strengths. Hence, *pH* 8 was chosen to be the optimal modification condition.

3.1.2. Ionic Strength Effect. In addition to the pH effect, the ionic strength is one of the most effective parameters that influences to the adsorption capacity. The electrolyte shielding effect prevents the hydrophilic interactions and promote the hydrophobic interactions [36–38]. The Γ_{PVBTAC} on the α-Al_2O_3 particles was determined at the four NaCl concentrations of 1, 10, 100 and 150 mM at *pH* 8, PVBTAC initial concentration of 50 ppm, contact time of 2 h and a α-Al_2O_3 adsorbent dosage of 5 mg mL^{-1}.

As obviously seen in Figure 3, the Γ_{PVBTAC} increased with increasing the NaCl concentration from 1 to 100 mM and decreases with continuous salt increment. It was subjected to contributions of different interaction kinds on the PVBTAC adsorption such as electrostatic interactions, including electrostatic attraction and electrostatic repulsion, and non-electrostatic interactions such as hydrogen bonding and Van der Waals. The Van der Waals not only between PVBTAC and the α-Al_2O_3 particles, but also between PVBTAC molecules, might take responsibility for the Γ_{PVBTAC} increment as the NaCl concentration went up from 1 to 100 mM. On the other hand, the electrolyte ions screened the electrostatic attraction between PVBTAC and the absorbent, the Γ_{PVBTAC} quickly dropped while the NaCl concentration passed 100 mM. A maximum Γ_{PVBTAC} of 3.24 mg g^{-1} was obtained at NaCl 100 mM. Hence, the ionic strength of 100 mM NaCl was employed to modify the α-Al_2O_3 surface.

3.1.3. PVBTAC Initial Concentration Effect. The polycation initial concentration effect on the α-Al_2O_3 modification efficiency was examined with the PVBTAC initial concentration from 25 to 1000 ppm at *pH* 8, NaCl 100 mM, contact time of 2 h. As shown in Figure 4, the Γ_{PVBTAC} considerably raised from 2.46 to 37 mg g^{-1} by increasing the PVBTAC

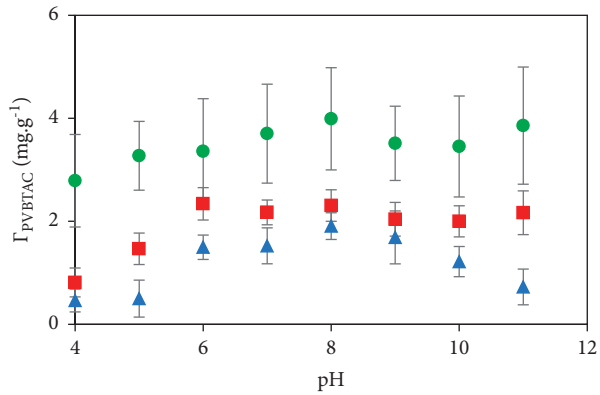

Figure 2: *pH* effect on the PVBTAC adsorption on the α-Al_2O_3 particles in different ionic strengths: (▲) 1 mM, (■) 10 mM and (●) 100 mM NaCl with $C_{i,PVBTAC}$ of 50 ppm, t of 2 h and $m_{\alpha\text{-}Al2O3}$ of 5 mg mL^{-1}.

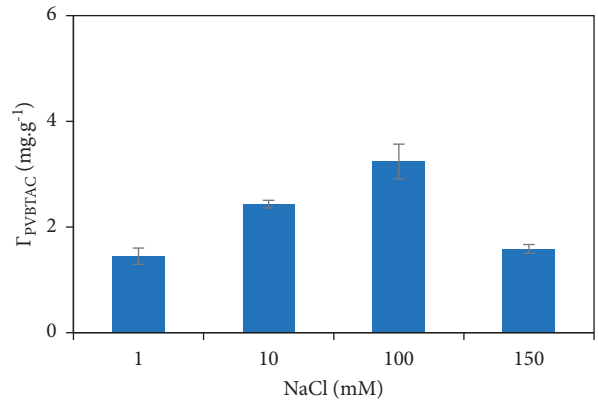

Figure 3: Ionic strength effect on the PVBTAC adsorption on the α-Al_2O_3 particles at *pH* 8, $C_{i,PVBTAC}$ of 50 ppm, t of 2 h and $m_{\alpha\text{-}Al2O3}$ of 5 mg mL^{-1}.

initial concentration in the range of 25–1000 ppm. The results can infer that more PVBTAC molecules were diffused and attached to the α-Al_2O_3 surface, due to main electrostatic interactions at high PVBTAC initial concentration and vice versa [38]. For the next experiments, the PVBTAC initial concentration of 1000 ppm was used to sufficiently modify the α-Al_2O_3 surfaces.

Summarily, the α-Al_2O_3 particle modification through PVBTAC adsorption was optimized at *pH* 8, ionic strength of 100 mM, contact time of 2 h, and PVBTAC initial concentration of 1000 ppm.

3.2. NCC Adsorptive Removal by Using PVBTAC-Modified α-Al_2O_3 Particles Confirmed by FT-IR Measurement. The successful α-Al_2O_3 surface modification by adsorbing polycation PVBTAC, and the NCC dye adsorptive removal through adsorption onto the PVBTAC-modified particles were confirmed based on the changes of functional groups determined by FT-IR spectroscopy. Formerly, the PVBTAC adsorption onto the α-Al_2O_3 particles was affirmed by comparing the FT-IR spectra of the pure α-Al_2O_3 particles

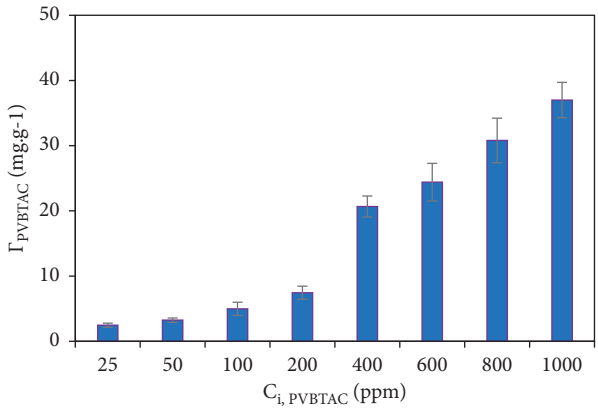

FIGURE 4: Initial concentration effect on the PVBTAC adsorption on the α-Al_2O_3 particles at pH 8, NaCl 100 mM, t of 2 h and $m_{\alpha\text{-Al2O3}}$ of 5 mg mL^{-1}.

and the pure PVBTAC with the PVBTAC-modified α-Al_2O_3 particle spectrum (Figure 5). The Al-O vibration of the α-Al_2O_3 was attributed at 446, 552, 582, 702, and 756 cm^{-1} [39] while a sharp peak of Al-OH vibration was obtained at 1051 cm^{-1} [40]. At the investigated pH 8 and NaCl 100 mM, O^-, O, and OH groups existed on the α-Al_2O_3 surface while only $-N^+R_3$ specified for PVBTAC (R abbreviating for $-CH_3$). Hence, the functional group vibrations will change if the interactions happen. The sharp peak at 1051 cm^{-1} presenting for the Al-OH vibration of the α-Al_2O_3 moved to 1059 cm^{-1} in the PVBTAC-modified α-Al_2O_3 spectrum. Besides, R_3N^+-C vibration arose at 1853, 2924, 3050, and 3360 cm^{-1} and especially, a strong band at 976 cm^{-1} assigned to C-N^+R_3 in the PVBTAC spectrum, disappeared in the PVBTAC-modified α-Al_2O_3 particle spectrum [41, 42]. These changes recognize the electrostatic attractions between amide in the PVBATC molecule and O^- the α-Al_2O_3.

Lately, the $S = O$ vibration at 1173 and 1144 cm^{-1} and the symmetrical $-SO_3^-$ stretching vibration at 1040 cm^{-1} of the NCC molecule disappeared in the PVBTAC-modified α-Al_2O_3 spectrum [43–45]. In addition to that, the R_3N^+-C vibration at 1800–3400 cm^{-1} and C-N peak at 976 cm^{-1} of PVBTAC in the spectrum of NCC-adsorbed-PVBTAC-modified α-Al_2O_3 [41, 42] were absent, strongly confirming the electrostatic attractions between $-SO_3^-$ of NCC and $-N^+R_3$ of PVBTAC. At the optimal *pH* 8 and NaCl 10 mM, the –OH group in the NCC was partly transferred to OH_2^+ as the pK_a is 11.38 [46], reducing its total negative charges as well as the electrostatic repulsion between the NCC molecules. We might imply that hydrogen bonding was formed among –OH groups between the NCC molecules because the peak at 3399 cm^{-1} corresponding to –OH vibration in the NCC molecule, disappeared in the spectrum of NCC-adsorbed-PVBTAC-modified α-Al_2O_3 [16, 44].

3.3. NCC Removal by Using the PVBTAC-modified α-Al_2O_3 Particles

3.3.1. Ionic Strength Effect. The removal efficiency of 10 ppm initial NCC concentration was more significantly enhanced by using the PVBTAC-modified α-Al_2O_3 adsorbents compared with using the unmodified nanosized α-Al_2O_3 particles at the same ionic strength of 10 mM NaCl and all *pH* (Figure 6). The modification of the α-Al_2O_3 adsorbents by PVBTAC adsorption improved the surface net charge, inducing additional electrostatic attractions between the positively charged PVBTAC covered on the α-Al_2O_3 surfaces and the negatively charged NCC molecules. Following this, the common effect factors to optimize the NCC removal through adsorbing onto the PVBTAC-modified α-Al_2O_3 adsorbents were comprehensively investigated.

As represented in Figure 6, two trends of the ionic strength effect on the NCC removal efficiency were observed. First, the ionic strength increment from 0 to 10 mM NaCl impulsed the NCC removal efficiency through adsorption onto the PVBTAC-modified α-Al_2O_3 particles at all *pH*. It can be explained that the promotion of the hydrogen bonding, and limitation of electrostatic repulsion between the NCC molecules, due to the condenser presence of electrolyte ions mainly controlled the NCC adsorption. However, the NCC removal efficiency decreased as the salt concentration was higher than 100 mM NaCl. The phenomenon suggested the significant shielding electrolyte ion effect on screening the electrostatic attractions between $-N^+R_3$ of the PVBTAC and $-SO_3^-$ of the dye NCC. It was consistent with our previous findings [36–38]. Herein, the NCC removal efficiency strongly depended on the interaction types between the NCC molecules and the PVBTAC-modified α-Al_2O_3 surface. Therefore, in all experiments, the ionic strength was controlled at NaCl 10 mM because the removal efficiency of the NCC was up to approximately 96% at almost all pH, and the standard deviation was lowest.

3.3.2. pH Effect. As could be seen in Figure 7, the NC removal efficiency, H_{NCC} and the adsorption amount, Γ_{NCC} unremarkably changed with the wide change of *pH* from 3 to 12. PVBTAC is highly positively charged and independent on *pH*. Normally, the –OH group of the NCC molecule more becomes $-OH_2^+$ in lower *pH*, reducing the NCC net negative charge. As a result, the electrostatic attraction between PVBCTAC and NCC is less strong at low *pH* than at high *pH*. However, as observed, the OH_2^+ formation contribution was negligible at pH lower than pK_a of NCC (pK_a 11.38) [46]. It is suggested that the NCC net charge was mainly decided by the sulfate groups. On the other hand, at the same salt concentration, the Γ_{NCC} got maximum at *pH* 8. The NCC removal was carried out at *pH* 8 and 10 mM NaCl.

3.3.3. Absorbent Dosage Effect. Normally, the total specific area significantly rises with an increment of absorbent dosage, enhancing more effectively adsorptive removal. The removal efficiency gradually changed from 53.94% to 99.25% with a 12-fold increment of the α-Al_2O_3 adsorbent dosage from 0.25 to 3 mg mL^{-1} (Figure 8). Then it was noticeably unchanged at the adsorbent dosage over 3 mg mL^{-1}. Herein, the adsorbent amount of 3 mg mL^{-1} was sufficient for the adsorptive removal of NCC.

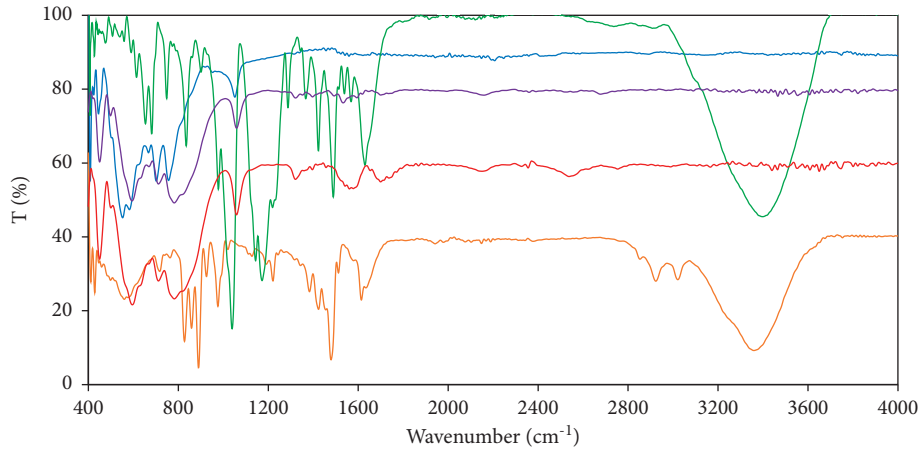

Figure 5: FT-IR spectra of: (—) α-Al2O3 particles, (—) polycation PVBTAC, (—) azo dye NCC, (—) PVBTAC-modified α-Al2O3 particles and (—) NCC-adsorbed-PVBTAC-modified α-Al2O3 particles.

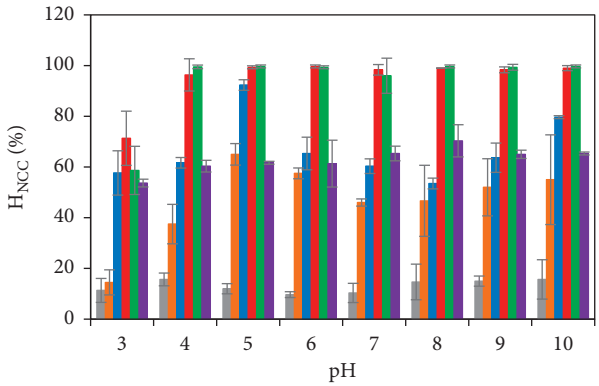

Figure 6: Ionic strength effect on the NCC adsorption onto the α-Al_2O_3 particles: without PVBTAC modification at (■) 10 mM NaCl and with PVBTAC modification at: (■) 0, (■) 1, (■) 10, (■) 100 and (■) 200 mM NaCl. Other conditions are $C_{i,\,NCC}$ of 10 ppm, t of 2 h, and $m_{\alpha\text{-Al2O3}}$ of 5 mg mL^{-1}.

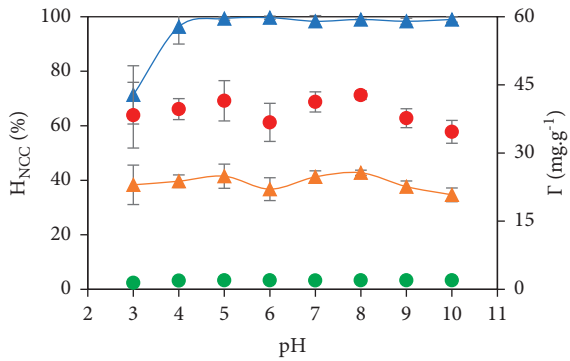

Figure 7: pH effect on the NCC adsorption onto the PVBTAC-modified α-Al_2O_3 particles at pH 8, NaCl 10 mM, t of 2 h and different conditions as $C_{i,NCC}$ of 10 ppm, $m_{\alpha\text{-Al2O3}}$ of 3 mg mL^{-1}: (▲) H_{NCC} (blue grid line) and (●) Γ_{NCC} (points); and $C_{i,NCC}$ of 100 ppm, $m_{\alpha\text{-Al2O3}}$ of 1 mg mL^{-1}: (▲) H_{NCC} (orange grid line) and (●) Γ_{NCC} (points).

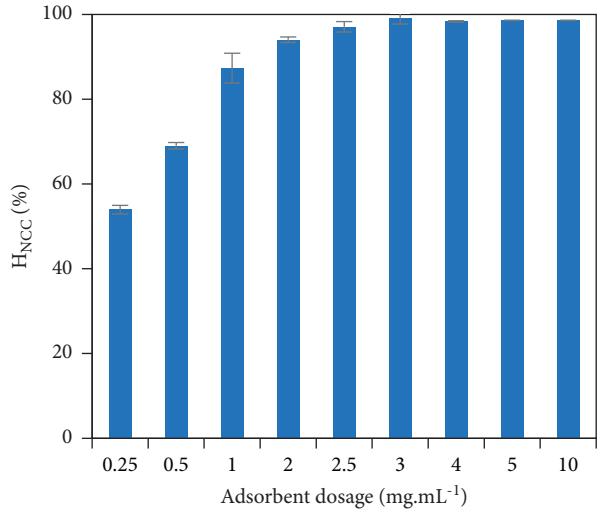

Figure 8: Effects of absorbent dosage on the NCC adsorption onto the PVBTAC-modified α-Al_2O_3 particles with $C_{i,NCC}$ of 10 ppm, pH 8, NaCl 10 mM, t of 2 h, and $m_{\alpha\text{-Al2O3}}$ of 3 mg mL^{-1}.

3.3.4. Contact Time Effect. The contact time effect on the NCC removal efficiency can be clearly observed in Figure 9. The NCC removal efficiency raised rapidly in each 15 min of the first 30 min. In the contact time range of 30–45 min, the removal efficiency continuously slowly raised from 96.25 to 97.40%. Then the removal efficiency was kept constant at the high removal efficiency of about 96% from 45 min to 120 min of the contact time. Accordingly, the NCC adsorption on the PVBTAC-modified α-Al_2O_3 surface reached an equilibrium state at the contact time of 45 min. Therefore, the optimal contact time of 45 min was applied for the next investigation.

3.3.5. NCC Adsorption Isotherm Model. The fitness of the NCC adsorption on the PVBTAC-modified α-Al_2O_3 particles with Langmuir, Freundlich and two-step models was examined. It can be seen clearly in Figure 10 that Γ_{NCC}

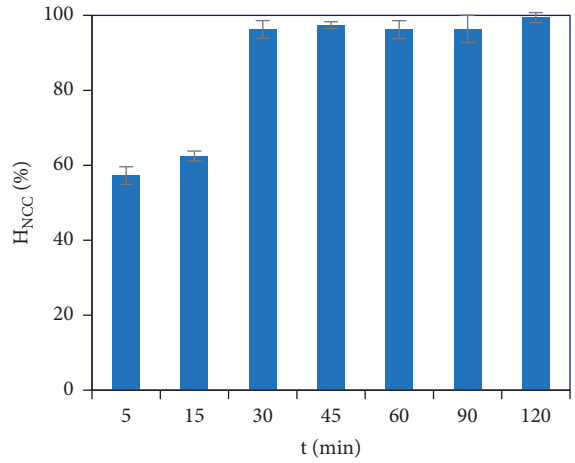

Figure 9: Effects of the absorbate dosage on the NCC adsorption onto the PVBTAC-modified α-Al_2O_3 particles with $C_{i,NCC}$ of 10 ppm, *pH* 8, NaCl 10 mM and $m_{\alpha\text{-}Al2O3}$ of 3 mg mL^{-1}.

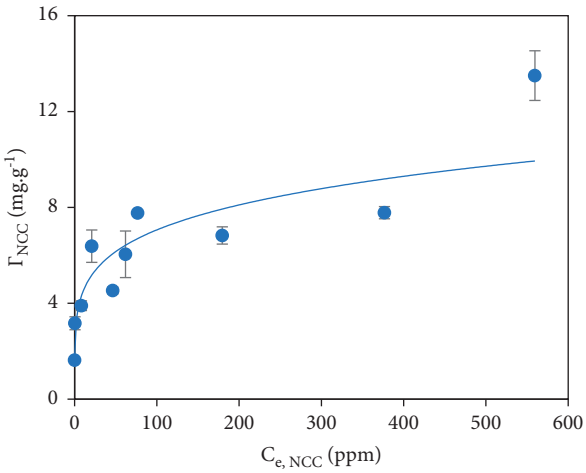

Figure 10: NCC adsorption on the PVBTAC-modified α-Al_2O_3 particles was well fitted with Freundlich model at conditions: $C_{i,NCC}$ from 10 to 600 ppm, *pH* 8, NaCl 10 mM, *t* of 45 min, and m_{α}-Al_2O_3 of 3 mg mL^{-1}.

gradually raised from about 1.62 to 13.5 mg g^{-1} as the NCC initial concentration increased from 5 to 600 ppm. A maximum NCC adsorption capacity of 13.5 mg g^{-1} determined proves that PVBTAC-modified α-Al_2O_3 was high-performance adsorbents in the NCC removal compared with other materials. The NCC adsorption capacity by using PVBTAC-modified α-Al_2O_3 particles was higher than using activated carbon as adsorbents (Table 1) [47–49]. Moreover, it might suggest that more numerous surface sites were available for NCC adsorption at low NCC initial concentration, intensifying the electrostatic attractions between NCC and adsorbed PVBTAC. Oppositely, the repulsive interactions between the NCC molecules were dominant at high NCC initial concentration. The NCC adsorptive removal only followed the Freundlich model with the fitting parameters calculated as K_f of 2.8341 and n of 0.1983 and not adapted with the Langmuir and two-step models (Figure 10).

3.3.6. NCC Adsorption Kinetics on PVBTAC-Modified α-Al_2O_3 Particles. Two kinetic models including pseudo-first and pseudo-second were considered for the NCC adsorption on PVBTAC-modified α-Al_2O_3 particles, as indicated in Figure 11.

The NCC adsorption kinetics on the PVBTAC-modified α-Al_2O_3 surface were better followed with the pseudo-second model with a higher correlation coefficient (R^2) of 0.9964 than the pseudo-first model with a lower R^2 of 0.7972 (Figure 11). It was proposed that there were some interactions between the adsorbed NCC molecules. In detail, the interactions might be resulted from hydrogen bondings between −OH groups in the NCC suggested by the FT-IR spectra above. The fitted parameters were shown in Table 2.

3.3.7. Regeneration of α-Al_2O_3 Adsorbent. Formerly, acidic solutions of 1, 2, 5 and 10 M HCl were used to regenerate α-Al_2O_3 adsorbent after the NCC adsorption. The regeneration procedure of the α-Al_2O_3 adsorbent was conducted twice. For each time, the PVBTAC-modified α-Al_2O_3 particles adsorbed the NCC were shaken with desired HCl concentration for 45 min. Then the concentration of the NCC desorbed was determined by the UV-Vis method at the wavelength of 508 nm. As shown in Figure 12, the NCC desorption efficiency in the first HCl treatment was low. After HCl treatment twice, the NCC adsorption efficiency reached higher than 90% at all HCl concentration. Moreover, the NCC desorption efficiency slightly raised with increasing 2-fold HCl concentration from 1 to 2 M, and reached maximum (approximately 97%) at the HCl higher than 5 M. It was referred to elute almost the NCC from the adsorbent surface. More presence of OH_2^+ groups on the particle surface under acidic condition led to stronger electrostatic repulsion between the positively charged PVBTAC and the positively charged α-Al_2O_3. As a result, the NCC were desorbed. Therefore, the regeneration of the α-Al_2O_3 adsorbent was carried out twice by using the HCl solution of 5 M. Each procedure of the HCl treatment twice was considered to be a regeneration time. The regeneration treatment of the α-Al_2O_3 adsorbents with strong acid at high concentration confirmed strong interactions between NCC and PVBTAC-modified surface, and the high synthesized adsorbent stability.

Lately, the regenerated α-Al_2O_3 particles were modified by the PVBTAC adsorption. Then the PVBTAC-modified-regenerated adsorbents were applied to adsorptively remove NCC. It was seen in Figure 13 that the NCC removal efficiency by using PVBTAC-modified-regenerated adsorbents decreased with rising the regeneration time. However, the NCC removal efficiency, achieved about 53% after four regeneration times, still was high. It was clarified that high reusability of the α-Al_2O_3 adsorbents.

Table 1: NCC adsorption capacities and NCC removal efficiencies by using different adsorbents.

Adsorbents	Adsorption capacity (mg g^{-1})	Removal efficiency (%)	References
PVBTAC-modified α-Al_2O_3	13.5	97.5	This study
Chemically treated mangrove barks	12.72	25.40	[47]
Activated carbon prepared from poplar woods	3.91	31.28	[48]
Activated carbon prepared from almond shells	10.75	90.83	[49]

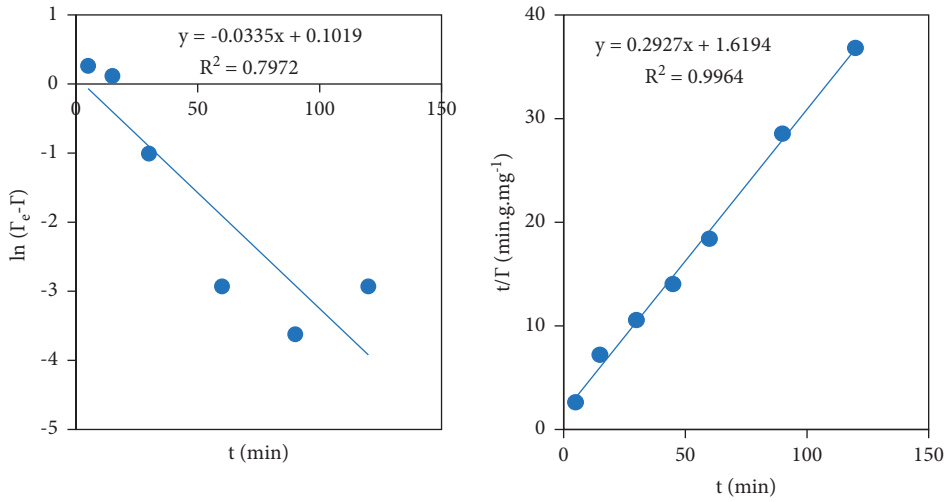

Figure 11: Kinetics of the PVBTAC adsorption isotherm on the α-Al_2O_3 particles following (a) pseudo-first and (b) pseudo-second at conditions of $C_{i,\ NCC}$ of 10 ppm, pH 8, NaCl 10 mM, and $m_{\alpha\text{-}Al2O3}$ of 3 mg mL^{-1}.

Table 2: Fitting parameters for the NCC adsorption onto the PVBTAC-modified α-Al_2O_3 particles following the pseudo-first and pseudo-second kinetic.

Parameters	Γ_e (mg.g^{-1})	R^2	K_1 (min^{-1})	K_2 (g mg^{-1} min^{-1})
Pseudo-first kinetic	3.21	0.7972	0.0335	
Pseudo-second kinetic	3.21	0.9964	-	0.0600

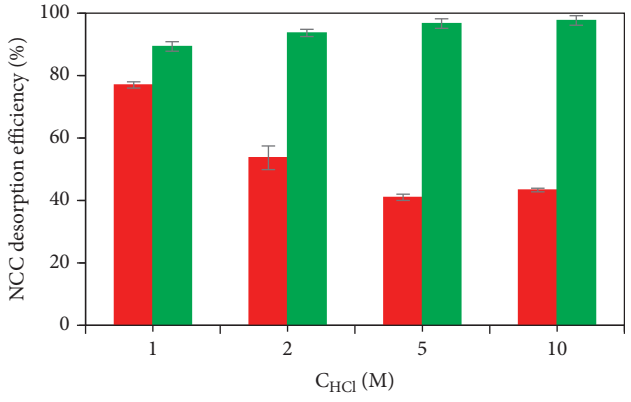

Figure 12: Effect of the HCl concentration to regenerate α-Al_2O_3 adsorbent with different HCl treatment times: (■) 1st and (■) 2nd.

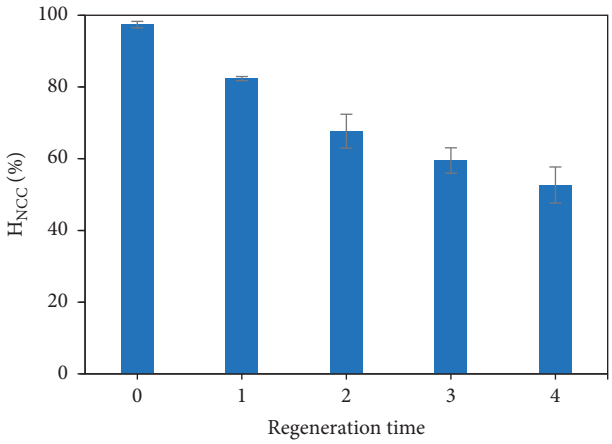

Figure 13: The NCC removal efficiency by adsorbing onto the PVBTAC-modified-regenerated α-Al_2O_3 adsorbents with different regeneration times at optimal conditions of: $C_{i,NCC}$ of 10 ppm, *pH* 8, NaCl 10 mM, and $m_{\alpha\text{-}Al2O3}$ of 3 mg mL^{-1}.

4. Conclusions

In the present study, it was the first time the azo dye NCC was highly adsorptively removed from aqueous solutions by using the PVBTAC polycation-modified α-Al_2O_3 particles. Both PVBTAC adsorption and NCC adsorption were comprehensively investigated. To sufficiently modify the α-Al_2O_3 particles, polycations PVBTAC of 1000 ppm initial concentration were adsorbed onto α-Al_2O_3 for 2 h at *pH* 8 under ionic strength of NaCl 100 mM. Then, the NCC adsorption on the PVBTAC-modified α-Al_2O_3 particles was optimized at conditions including *pH* 8, NaCl 10 mM, contact time of 45 min, and an α-Al_2O_3 dosage of 3 mg g^{-1}. The adsorption of both PVBTAC and NCC was controlled by the electrostatic and non-interaction that also affirmed by the FT-IR spectra. The mechanism and kinetics of the NCC adsorption isotherm onto the PVBTAC-modified α-Al_2O_3 particles were clarified. The NCC adsorption isotherm mechanism was in accordance with the Freundlich model, while the NCC adsorption kinetics was more suitably followed by the pseudo-second than the pseudo-first model. The nanosized alpha alumina was proved to be a highly reusable adsorbent.

Data Availability

All the data and supporting materials are included within the article.

Conflicts of Interest

All authors declare that there are no conflicts of interest regarding the publication of this paper.

Acknowledgments

Dr. Thi Hai Yen Doan would like to thank Prof. Shin-ichi Yusa, University of Hyogo, Japan, for supporting polymer materials and Dr. Johan Hunziker, Kobe University, Japan for the available comments and English check to improve our manuscript.

References

[1] A. G. R Ananthashankar, "Production, characterization and treatment of textile effluents: a critical review," *Journal of Chemical Engineering & Process Technology*, vol. 05, no. 01, 2013.

[2] P. Kalyani, "Degradation of toxic dyes-A review," *International Journal of Pure & Applied Bioscience*, vol. 4, pp. 81–89, 2016.

[3] D. A. Yaseen and M. Scholz, "Textile dye wastewater characteristics and constituents of synthetic effluents: a critical review," *International journal of Environmental Science and Technology*, vol. 16, no. 2, pp. 1193–1226, 2019.

[4] B. d. C. Ventura-Camargo and M. A. Marin-Morales, "Azo dyes: characterization and toxicity–A review," *Textiles and Light Industrial Science and Technology*, vol. 2, 2013, https://www.researchgate.net/publication/282815745_Azo_Dyes_Characterization_and_Toxicity-_A_Review.

[5] K.-T. Chung, "Azo dyes and human health: a review," *Journal of Environmental Science and Health, Part C*, vol. 34, no. 4, pp. 233–261, 2016.

[6] B. Lellis, C. Z. Fávaro-Polonio, J. A. Pamphile, and J. C. Polonio, "Effects of textile dyes on health and the environment and bioremediation potential of living organisms," *Biotechnology Research and Innovation*, vol. 3, no. 2, pp. 275–290, 2019.

[7] A. Ahmad, S. H. Mohd-Setapar, C. S. Chuong et al., "Recent advances in new generation dye removal technologies: novel search for approaches to reprocess wastewater," *RSC Advances*, vol. 5, no. 39, pp. 30801–30818, 2015.

[8] S. Papić, N. Koprivanac, A. L. Božić et al., "Advanced oxidation processes in azo dye wastewater treatment," *Water Environment Research*, vol. 78, no. 6, pp. 572–579, 2006.

[9] S. Ledakowicz and K. Paździor, "Recent achievements in dyes removal focused on advanced oxidation processes integrated with biological methods," *Molecules*, vol. 26, no. 4, p. 870, 2021.

[10] A. G. Liew Abdullah, M. Salleh, M. K. S. Mazlina et al., "Azo dye removal by adsorption using waste biomass: sugarcane bagasse," *International Journal of Engineering and Technology*, vol. 2, pp. 8–13, 2005, https://www.researchgate.net/publication/238086341_Azo_dye_removal_by_adsorption_using_waste_biomass_Sugarcane_bagasse.

[11] R. G. Saratale, G. D. Saratale, J. S. Chang, and S. P. Govindwar, "Bacterial decolorization and degradation of azo dyes: a review," *Journal of the Taiwan Institute of Chemical Engineers*, vol. 42, no. 1, pp. 138–157, 2011.

[12] M. Chen, W. Ding, J. Wang, and G. Diao, "Removal of azo dyes from water by combined techniques of adsorption, desorption, and electrolysis based on a supramolecular sorbent," *Industrial & Engineering Chemistry Research*, vol. 52, no. 6, pp. 2403–2411, 2013.

[13] G. Ranalli, P. Principi, and C. Sorlini, "Bacterial aerosol emission from wastewater treatment plants: culture methods and bio-molecular tools," *Aerobiologia*, vol. 16, no. 1, pp. 39–46, 2000.

[14] L. Wang, Y. Han, and L. Li, "Degradation of acid red 18 by Fenton reagent combined with UV," *Asian Journal of Chemistry*, vol. 22, pp. 6693–6700, 2010.

[15] S. Wang, Y.-Y. Zhai, Q. Gao, W.-J. Luo, H. Xia, and C.-G. Zhou, "Highly efficient removal of acid red 18 from

aqueous solution by magnetically retrievable chitosan/carbon nanotube: batch study, isotherms, kinetics, and thermodynamics," *Journal of Chemical & Engineering Data*, vol. 59, no. 1, pp. 39–51, 2014.

[16] A. A. Najafi Chaleshtori, F. M. Meghadddam, M. M. Sadeghi, R. R. Rahimi, S. Hemati, and A. A. Ahmadi, "Removal of acid red 18 (Azo-dye) from aqueous solution by adsorption onto activated charcoal prepared from almond shell," *Journal of Environmental Science and Management*, vol. 20, pp. 9–16, 2017, https://www.researchgate.net/publication/323837665_Removal_of_acid_red_18_Azo-dye_from_aqueous_solution_by_adsorption_onto_activated_charcoal_prepared_from_almond_shell.

[17] M. Shirmardi, A. Mesdaghinia, A. H. Mahvi, S. Nasseri, and R. Nabizadeh, "Kinetics and equilibrium studies on adsorption of acid red 18 (Azo-Dye) using multiwall carbon nanotubes (MWCNTs) from aqueous solution," *E-Journal of Chemistry*, vol. 9, no. 4, pp. 2371–2383, 2012.

[18] M. R. Samarghandi, M. Zarrabi, A. Amrane et al., "Kinetic of degradation of two azo dyes from aqueous solutions by zero iron powder: determination of the optimal conditions," *Desalination and Water Treatment*, vol. 40, no. 1–3, pp. 137–143, 2012.

[19] J. W. Ntalikwa, "Determination of surface charge density of α-alumina by acid-base titration," *Bulletin of the Chemical Society of Ethiopia*, vol. 21, no. 1, 2007.

[20] J. P. Maher, "Chapter 4. Aluminium, Gallium, Indium and Thallium," *Annual Reports Section "A" (Inorganic Chemistry)*, vol. 93, pp. 45–58, 1997.

[21] T. Feininger, "Rock-forming minerals. 5A. Non-silicates: oxides, hydroxides, and sulphides (2nd edition)," *The Canadian Mineralogist*, vol. 495, pp. 1335-1336, 2nd edition, 2011.

[22] T. D. Pham, M. Kobayashi, and Y. Adachi, "Adsorption characteristics of anionic azo dye onto large α-alumina beads," *Colloid & Polymer Science*, vol. 293, no. 7, pp. 1877–1886, 2015.

[23] T. D. Pham, M. Kobayashi, and Y. Adachi, "Adsorption of anionic surfactant sodium dodecyl sulfate onto alpha alumina with small surface area," *Colloid & Polymer Science*, vol. 293, no. 1, pp. 217–227, 2015.

[24] T. D. Pham, T. T. Tran, V. A. Le, T. T. Pham, T. H. Dao, and T. S. Le, "Adsorption characteristics of molecular oxytetracycline onto alumina particles: the role of surface modification with an anionic surfactant," *Journal of Molecular Liquids*, vol. 287, Article ID 110900, 2019.

[25] S. A. C. Carabineiro, T. Thavorn-Amornsri, M. F. R. Pereira, and J. L. Figueiredo, "Adsorption of ciprofloxacin on surface-modified carbon materials," *Water Research*, vol. 45, no. 15, pp. 4583–4591, 2011.

[26] T.-H. Dao, T.-Q.-M. Vu, N.-T. Nguyen et al., "Adsorption characteristics of synthesized polyelectrolytes onto alumina nanoparticles and their application in antibiotic removal," *Langmuir*, vol. 36, no. 43, pp. 13001–13011, 2020.

[27] T. T. T. Truong, T. N. Vu, T. D. Dinh et al., "Adsorptive removal of cefixime using a novel adsorbent based on synthesized polycation coated nanosilica rice husk," *Progress in Organic Coatings*, vol. 158, Article ID 106361, 2021.

[28] T. D. Pham, V. P. Bui, T. N. Pham et al., "Adsorptive removal of anionic azo dye new coccine using silica and silica-gel with surface modification by polycation," *Polymers*, vol. 13, no. 10, p. 1536, 2021.

[29] M. Shabandokht, E. Binaeian, and H.-A. Tayebi, "Adsorption of food dye Acid red 18 onto polyaniline-modified rice husk composite: isotherm and kinetic analysis," *Desalination and Water Treatment*, vol. 57, pp. 1–13, 2016.

[30] X. Li, A. Li, M. Long, and X. Tian, "Equilibrium and kinetic studies of copper biosorption by dead Ceriporia lacerata biomass isolated from the litter of an invasive plant in China," *Journal of Environmental Health Science and Engineering*, vol. 13, no. 1, pp. 1–8, 2015.

[31] M. Kuczajowska-Zadrożna, U. Filipkowska, U. Filipkowska, T. Jóźwiak, and P. Szymczyk, "The use of polysaccharides for acid red 18 anionic dye removal from aqueous solutions," *Progress on Chemistry and Application of Chitin and its Derivatives*, vol. 22, pp. 106–117, 2017.

[32] Z. Liu and K. Xing, "Removal of acid red 88 using activated carbon produced from pomelo peels by KOH activation: orthogonal experiment, isotherm, and kinetic studies," *Journal of Chemistry*, vol. 2021, Article ID 6617934, 9 pages, 2021.

[33] L. Zhang and F. Wang, "Kinetics and characteristics studies on biosorption of acid red 18 from aqueous solution by the acid-treated mycelia pellets of Penicillium janthinellum," *Desalination and Water Treatment*, vol. 167, pp. 313–323, 2019.

[34] N. T. Nguyen, T. H. Dao, T. T. Truong, T. M. T. Nguyen, and T. D. Pham, "Adsorption characteristic of ciprofloxacin antibiotic onto synthesized alpha alumina nanoparticles with surface modification by polyanion," *Journal of Molecular Liquids*, vol. 309, Article ID 113150, 2020.

[35] T. D. Pham, M. Kobayashi, and Y. Adachi, "Interfacial characterization of α-alumina with small surface area by streaming potential and chromatography," *Colloids and Surfaces A: Physicochemical and Engineering Aspects*, vol. 436, pp. 148–157, 2013.

[36] T. H. Y. Doan, T. D. Pham, J. Hunziker, and T. H. Hoang, "Temporal changes of adsorbed layer thickness and electrophoresis of polystyrene sulfate latex particles after long incubation of oppositely charged polyelectrolytes with different charge densities," *Polymers*, vol. 13, no. 15, p. 2394, 2021.

[37] T. H. Y. Doan, V. H. Lim, Y. Adachi, and T. D. Pham, "Adsorption of binary mixture of highly positively charged PTMA5M and partially negatively charged PAA onto PSL particles studied by means of brownian motion particle tracking and electrophoresis," *Langmuir*, vol. 37, no. 41, pp. 12204–12212, 2021.

[38] T. H. Y. Doan and Y. Adachi, "Relaxation of adsorbed layer thickness and electrophoresis of polystyrene latex particles after overshooting of polyelectrolytes with different charge density," *Colloids and Surfaces A: Physicochemical and Engineering Aspects*, vol. 603, Article ID 125208, 2020.

[39] A. Boumaza, A. Djelloul, and F. Guerrab, "Specific signatures of α-alumina powders prepared by calcination of boehmite or gibbsite," *Powder Technology*, vol. 201, no. 2, pp. 177–180, 2010.

[40] C. Ma, Y. Chang, W. Ye, W. Shang, and C. Wang, "Supercritical preparation of hexagonal γ-alumina nanosheets and its electrocatalytic properties," *Journal of Colloid and Interface Science*, vol. 317, no. 1, pp. 148–154, 2008.

[41] Y. Ji, X. Yang, Z. Ji et al., "DFT-calculated IR spectrum amide I, II, and III band contributions of N-methylacetamide fine components," *ACS Omega*, vol. 5, no. 15, pp. 8572–8578, 2020.

[42] M. S. Agashe and C. I. Jose, "Characteristic vibrations of -N(CH3)2and -N+(CH3)3groups in dimethyl aminophenols and their methiodides," *Journal of the Chemical Society, Faraday Transactions 2*, vol. 73, no. 7, pp. 1232–1237, 1977.

[43] S. B. Brijmohan, S. Swier, R. A. Weiss, and M. T. Shaw, "Synthesis and characterization of cross-linked sulfonated

polystyrene nanoparticles," *Industrial & Engineering Chemistry Research*, vol. 44, no. 21, pp. 8039–8045, 2005.

[44] C. O. M'Bareck, Q. T. Nguyen, M. Metayer, J. M. Saiter, and M. R. Garda, "Poly (acrylic acid) and poly (sodium styrenesulfonate) compatibility by Fourier transform infrared and differential scanning calorimetry," *Polymer*, vol. 45, no. 12, pp. 4181–4187, 2004.

[45] M. Wawrzkiewicz, B. Podkościelna, and P. Podkościelny, "Application of functionalized dvb-co-gma polymeric microspheres in the enhanced sorption process of hazardous dyes from dyeing baths," *Molecules*, vol. 25, no. 22, p. 5247, 2020.

[46] S. Ötles, *Handbook of Food Analysis Instruments*, CRC Press, Boca Raton, FL, USA, 2016.

[47] L. S. Tan and M. J. N. Kassim, "Acidic and basic dyes removal by adsorption on chemically treated mangrove barks," *International Journal of Applied Science and Technology*, vol. 2, pp. 270–276, 2012.

[48] R. Shokoohi, V. Vatanpoor, M. Zarrabi, and A. Vatani, "Adsorption of acid red 18 (AR18) by activated carbon from poplar wood- A kinetic and equilibrium study," *E-Journal of Chemistry*, vol. 7, no. 1, pp. 65–72, 2010.

[49] A. A. Najafi Chaleshtori, F. M. Meghadddam, M. M. Sadeghi, R. R. Rahimi, S. Hemati, and A. A. Ahmadi, "Removal of acid red 18 (Azo-dye) from aqueous solution by adsorption onto activated charcoal prepared from almond shell," *Journal of Environmental Science and Management*, vol. 20, pp. 9–16, 2017, https://ovcre.uplb.edu.ph/journals-uplb/index.php/JESAM/article/view/119.